The Magnitude Threshold for Detecting Recorded Earthquakes in Tehran's Accelerometer Networks

Masih, M.[1] | Kianimehr, H.[2] | Shomali, Z. H.[3] ✉ | Bayramnejad, E.[4]

1. Department of Seismology, Institute of Geophysics, University of Tehran, Tehran, Iran. E-mail: mehrasa.masih@ut.ac.ir
2. Iranian Seismological Center, Kerman, Iran. E-mail: kianimehrhossein@gmail.com
3. **Corresponding Author**, Department of Seismology, Institute of Geophysics, University of Tehran, Tehran, Iran. E-mail: shomali@ut.ac.ir
4. Department of Seismology, Institute of Geophysics, University of Tehran, Tehran, Iran. E-mail: ebayram@ut.ac.ir

Abstract

Due to the population growth in metropolitan regions such as Tehran and the existence of the underground constructions, the importance of seismic investigation is evident to reduce damages caused by probable earthquakes. Accordingly, the precise detection of micro to medium earthquakes is effective tool for tracking fault dynamics in seismic cycles, as well as for earthquake prediction and seismic hazard assessment. In this study, the recorded ambient noise at Tehran Disaster Mitigation and Management Organization (TDMMO) as well as Road, Housing and Urban Development Research Center (BHRC) networks as an accelerometer network installed in Tehran city, have been used on the point of characterizing the noise spectrum for each station as a function of time for obtaining the detection threshold of these networks. Therefore, an indirect approach based on the signal-to-noise ratio (SNR) in the time domain, with parameterization in the frequency domain is applied. Based on SNR method, the source signature is simulated by a simple source model called a circular fault model. Thus, the signal is estimated via the Brune function as most common models for circular faults. While, to determine the noise, the real data of 13 accelerometer stations of the TDMMO and seven joint stations with the BHRC are used. In this respect, the Power Spectral Density (PSD) of noise is calculated using PQLX software in the frequency domain and then is transferred to the time domain by the Parsville theorem. Eventually, the SNR value is acquired for each station by dividing these two quantities. As a result, the minimum detectable magnitude in at least five stations with an SNR larger than 5 is 3.0 for S-waves and 3.3 for P-waves, which frequently occurs in the center of the network.

Another finding of these studies is to analyze the effect of spatial variations of the noise on the detection ability. For this, a constant noise is allotted to all stations, lowest observed noise level, as a result of which, the smallest magnitude detectable is 1.7 for S-waves and 2.2 for P-waves.

At last, the sensitivity of the detection capability to three fundamental parameters, including stress drop, focal depth and reduced time, which are assumed as constant values within the network, are investigated. In fact, these parameters are strongly affected by uncertainty and are not absolute values. Consequently, the impact of their changes was studied. In our case, it is implied that the variation in the stress drop has no effect on the detection threshold, but the focal depth and the reduced time are effectual. A 15 km variation in the focal depth, the detectable magnitude changes by 0.3 units, and by changing the reduced time from 0.015 s to 0.035 s, the detectable magnitude varies by 0.4 units in M_w.

Keywords: Detection threshold, PSD, PQLX software, SNR, Spectrum.

1. Introduction

Seismology is a science based on collecting and analyzing seismic waves. Therefore, the role of seismic and accelerometer networks in the development of this science, and the human knowledge about the seismic characteristics of different regions of the earth is significant. As a consequence, in Iran, due to the need for more complete seismic information for advanced and accurate seismic studies, the number of seismic network stations in different places that continuously record the movement of the earth have been expanded. Determining the detection threshold, as a 90% probability of

detecting and localizing minimal magnitude events can be done using several methods, which can be usually traced in three basic techniques (Ringdal, 1975).

- The indirect estimation method based on the seismic noise studies. In this method, estimating the signal-to-noise-ratio is required for the detection, and by assuming a signal variance, the actual detection performance of a system can be reasonably predicted.

- The recurrence curve estimation method based on the seismicity as a two-step procedure. First, the seismicity of a region is estimated by extrapolating of the observed data, using the exponential magnitude-frequency relationship. Then, observed number of events is compared to the estimated seismicity to establish detection thresholds.

- The direct estimation method is based on comparison with a reference system. In this method, a set of events reported by an independent reference system is selected. After that, the percentage detected for each magnitude is then used to estimate thresholds.

2. Data and Method

In this research, Tehran metropolis has been chosen to determine the seismic detection threshold due to its location in the central part of the Alpine-Himalayan seismic belt and also being encompassed via numerous active faults with some reported M7+ historical earthquakes (Memarian et al., 2020). In general, the detection threshold can be defined as the minimum magnitude for which 90% of the events will be identified and localized (Vassallo et al., 2012). This detection is crucial for seismological purposes such as the earthquake prediction and seismic hazard assessment. The utilized approach in this study is based on the indirect signal-to-noise ratio (SNR) method and background noise analysis. Hence, used data is derived from the noise recorded in two accelerometer networks, Tehran Disaster Mitigation and Management Organization (TDMMO) and Road, Housing and Urban Development Research Center (BHRC), which are equipped with Guralp CMG-5T three-component accelerometers with a sampling frequency of 100 sample per second. These networks consist of 14 and 10 stations, respectively. However, just 13 stations of TDMMO and 7 ones of BHRC networks were usable during the time period used for this research (11-25 December 2020).

Table 1. The coordinate of accelerometer stations used in this study.

Number	Stations	Longitude (ºE)	Latitude (ºN)	Altitude (meter)	Reference
1	TDMM	51.339806	35.725020	1288	TDMMO
2	D221	51.201710	35.759230	1343	TDMMO
3	D211	51.146173	35.728940	1230	TDMMO
4	D201	51.424500	35.588100	-	TDMMO
5	D181	51.328693	35.651240	1137	TDMMO
6	D161	51.411620	35.63054	1114	TDMMO
7	D152	51.643310	35.52239	1042	TDMMO
8	D151	51.495358	35.62047	1173	TDMMO
9	D121	51.423253	35.685226	1180	TDMMO
10	D071	51.431648	35.726788	1304	TDMMO
11	D042	51.628200	35.738100	-	TDMMO
12	D041	51.541403	35.760243	1501	TDMMO
13	D011	51.464400	35.825100	-	TDMMO
14	D191	51.362781	35.634563	1104	BHRC
15	D141	51.463414	35.662221	1277	BHRC
16	D052	51.3222222	35.707222	1238	BHRC
17	D222	51.223000	35.754000	1300	BHRC
18	D131	51.483294	35.704804	1195	BHRC
19	D101	51.3754928	35.670886	1154	BHRC
20	D021	51.339479	35.73548	1276	BHRC

In this study, the indirect SNR method is used to evaluate the earthquake detection threshold by the accelerometer stations of the TDMMO jointly with the BHRC ones. According to this method, a simple source model, circular fault model, is used to simulate the signal. The Brune model, the most common model for finite dimensional circular faults, assumes a circular rupture, the radius of which determines the corner frequency. This model associates the spectrum of shear radiation to the released stress along the fault surface. The high frequency level of the source spectrum is controlled by the stress parameter, whereas its low-frequency level is proportional to the seismic moment (Atkinson, 1993). Generally, the model provides a simple interpretation of the observed spectra in terms of the moment magnitude and stress drop (Brune, 1970, 1971). Therefore, the near source spectrum can be considered as (Boore & Boatwright, 1984):

$$S(f) = \frac{R_{\theta\varphi} F_s M_0}{4\pi\rho\beta^3 R} \frac{(2\pi f)^2}{1+(\frac{f}{f_c})^2} e^{-\pi t^* f} \quad (1)$$

where $R_{\theta\varphi}$ is the radiation pattern which has an averaged value of 0.55 for the P-waves and S-waves because of an unknown focal mechanism (Boore and Boatwright, 1984); F_s, the free surface correction as a factor in the use of borehole data that is equal to 2 for the P- and S-waves (Malagnini & Dreger, 2016), M_0, seismic moment; f, frequency; φ, density; β, shear wave velocity; R, hypocentral distance; t^*, the travel time reduced by a quality factor, and f_c is the corner frequency. The values of this parameters in Tehran region are as follows (Zafarani et al., 2008):

$\rho = 2800$ kg.m^{-3} , $\beta = 3500$ m.s^{-1} , $\alpha = 6200$ m.s^{-1} .

In the Brune model, the attenuation of seismic waves is expressed by t^*. The attenuation properties of the Earth are represented by the quality factor, Q, as a measurement for the loss of seismic wave energy as it travels through the Earth. t^* represents the mean attenuation along the entire path that is considered by an integral over the ray path (Weidle et al., 2007) by a mean value of 0.025 sec for both P- and S-waves (Margheriti & Zollo, 2010).

The corner frequency is computed using a constant stress drop, $\Delta\sigma = 5\ Mpa$, according to Equation (2):

$$f_c = \frac{2.34}{2\pi}\beta\left(\frac{16}{7}\frac{\Delta\sigma}{M_0}\right)^{\frac{1}{3}} \quad (2)$$

According to the properties of Fourier transformation, an acceleration spectrum (Equation 1) has three characteristics: (a) increasing proportionally to f^2 in low frequencies ($f < f_c$), (b) at almost $f = f_c$ the amplitude begins to stabilize, and (c) a high frequency fixed section ($f > f_c$).
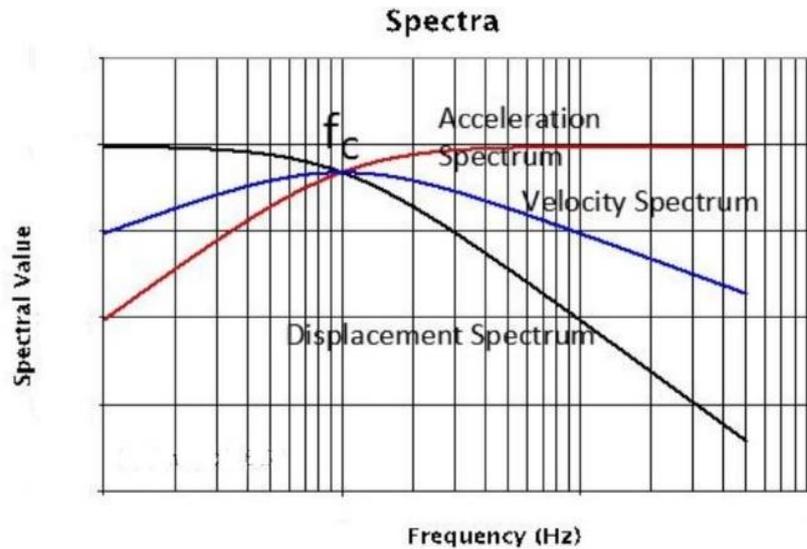
Figure 1. The schematic Fourier Amplitude Spectrum of strong earthquake acceleration (Ding, 2015).

The SNR's denominator, i.e. the background noise level, is determined using the power spectral density (PSD) for the TDMMO and BHRC stations. The PSD is calculated by all three components of the acceleration spectrum at frequency values in the at frequency ranges corresponding to the corner frequencies of earthquake by the PQLX software (Incorporated Research Institutions for Seismology, 2017). In this procedure, the data format conversion from gcf to miniseed is the first step and then the continuous time-series for each component at each station is divided into 1-hour segments with considering 50% overlap. To decrease the variation in the final PSD estimation, each one-hour time series is broken into 13 parts that are about 18 minutes long with 75% overlap in time. To prevent spectral processing distortions, mean and long-period trends must be removed in each segment, afterwards a 10% cosine taper is applied to minimize the effect of discontinuity between the beginning and the end of time series, and processing is performed using an FFT (Fast Fourier Transform) algorithm. Finally, each one-hour time series segment is averaged to obtain a PSD.

The estimated PSDs are used to produce the PDFs, which are valuable tools for examining the energy distribution over the seismic spectrum, and the monitoring temporal variations to determine the likelihood of background noise in each station as a function of period. In this regard, (1) Frequencies are averaged in 1/8 octave intervals, and (2) powers are aggregated in 1-dB bins to calculate the PDF for each period. The resultant frequency distribution in each bin is then normalized by the total number of computed PSDs to get a PDF for each period.

Concurring to the above clarifications, a sample of PSD-PDF maps acquired by the PQLX software for the Z component of the D191 station of Road, Housing and Urban Development Research Center and the TDMMO station of Tehran Disaster Mitigation and Management Organization in the duration of 15-December to 24-December 2020 as a function of distinctive periods are drawn in Figure 2.
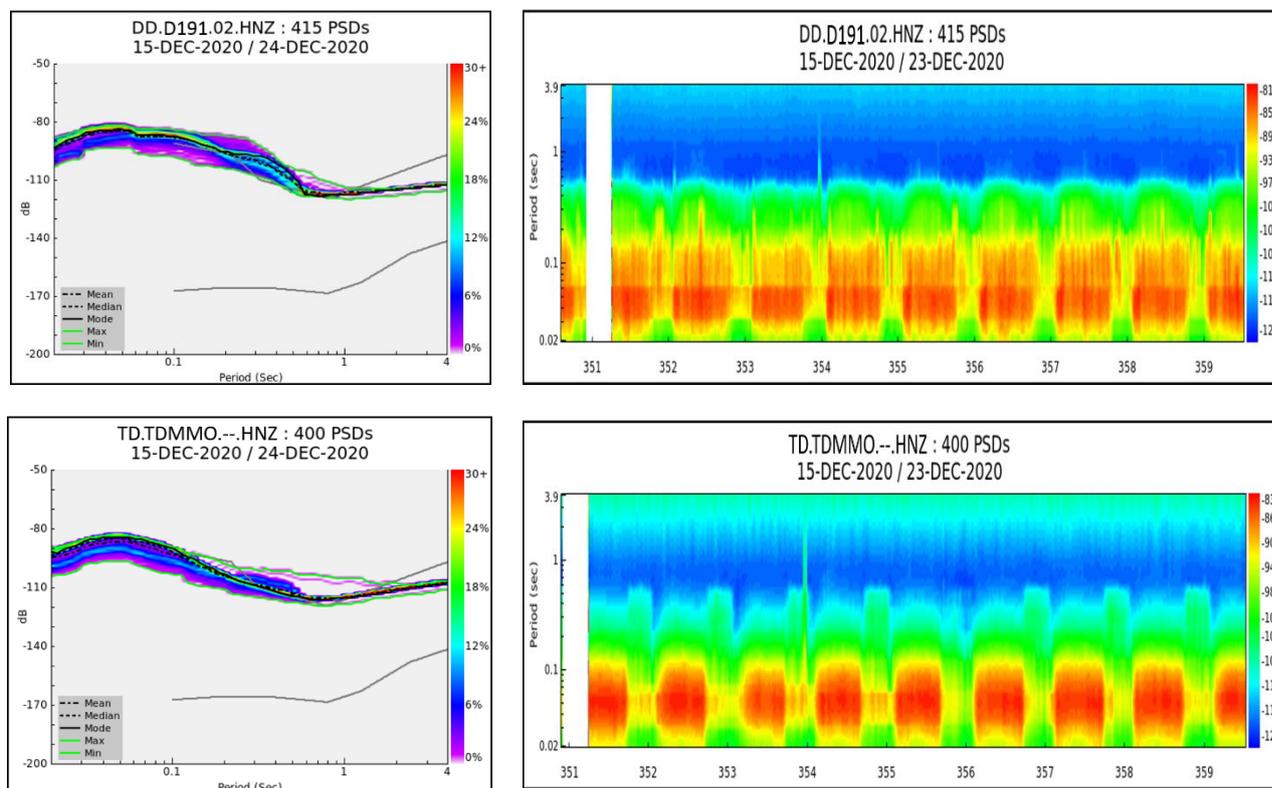
Figure 2. An example of the PSD-PDF maps for the vertical component of D191 (from the BHRC network) and TDMMO station.

Notably, the amplitude spectrum is not directly comparable with the PSD associated with noise. Hence, the detection threshold is parameterized as a function of the SNR in the time domain (Aki & Richards, 1980). For this purpose, the Brune spectrum is converted into a time domain function by separating the source effect from the anelastic attenuation, then the amplitude of signal in the time domain is obtained from the convolution of the attenuation coefficient and the Brune spectrum in the time domain (Equation 3).

$$S(t) = s_1(t) * s_2(t)$$

$$= M_0 \frac{2R_{\theta\phi}F_s f_c^2}{\rho R c^3 t^*}$$

$$\int_0^{+\infty} (1 - 2\pi f_c \tau) \times e^{-2\pi f_c \tau} \frac{t^{*2}}{t^{*2} + 4(t-\tau)^2} d\tau \qquad (3)$$

where S(t) is an odd function with a maximum at positive time values, the maximum of which, |S(t)|, is used as the SNR's numerator. To gauge the noise level in the time domain, the mean square amplitude of the noise in the time domain is computed using the PSD and the Parseval theorem in which the square integral of a function is equal to the square integral of its Fourier transform (Equation 4).

$$\left\langle \left| n(t) \right|^2 \right\rangle = 2 \int_{f_{min}}^{f_{max}} P(f)df = 2 \langle P(f) \rangle \left(f_{max} - f_{min} \right) \qquad (4)$$

where P(f) denotes the PSD; f_{max} is chosen 50 Hz on the basis of the acquisition sampling rate (100 sps); and f_{min} is 0.2 Hz to reduce the baseline effect generated by the long-period noise in the micro-seismic band.

Eventually, the SNR is calculated by dividing Equation (3) by (4).

$$SNR = M_0 C(f_c, t^*) \frac{2R_{\theta\phi}F_s f_c^2}{\rho R c^3 t^* \sqrt{2\langle P \rangle (f_{max} - f_{min})}} \qquad (5)$$

where $C(f_c, t^*)$ is equal to the maximum of the integral in Equation (3).

$$C(f_c, t^*) =$$

$$\max(\int_0^{+\infty} (1 - 2\pi f_c \tau) \times e^{-2\pi f_c \tau} \frac{t^{*2}}{t^{*2} + 4(t-\tau)^2} d\tau) \qquad (6)$$

Due to the dependence of the amplitude of P- and S-waves on an earthquake location, a regular network is defined in the study area. The investigation area is networked with cells of 1×1 km^2, and based on the average depth of most earthquakes in this region, the epicenter of the earthquake on each node of the network are considered at a depth of 10 km (Yazdani et al., 2016). After that, the smallest seismic moment associated with a seismic event recorded by at least five stations with an SNR > 5 is computed in each node. This ratio provides an accurate estimate of the local magnitude for those events recorded by the network. Hence, such a value is considered as the minimum requirement to identify the S- and P-phases on horizontal and vertical components, respectively (Bobbio et al., 2009). Finally, to estimate the detection threshold associated with each node, the seismic moment is converted into the moment magnitude according to the formula $M_w = 0.67 \log M_0 - 6.07$ (Vassallo et al., 2012).

3. Implementation of the method

Ultimately, by the mentioned method, the detection threshold maps for the studied area and P- and S- waves are plotted in Figure 3 via calculating the threshold magnitude for each node at a depth of 10 km.

These results imply that the smallest detectable magnitudes for the S- and P-waves are 3.0 and 3.3, respectively in the center of the network, and present the variation of noise levels at different stations (Figures 3-a, 3-b, 3-c). Therefore, the constant noise level is assigned to all stations within the network in order to evaluate the effect of the spatial variation of the noise on the detection capability. This consistent value is equal to the noise level of station D071, which almost experiences the minimum noise level in all the short period ranges. As a result of this assumption, the smallest magnitude detectable is 1.7 for S-waves and 2.2 for P-waves (Figure 4).

(a)

(b)

(c)
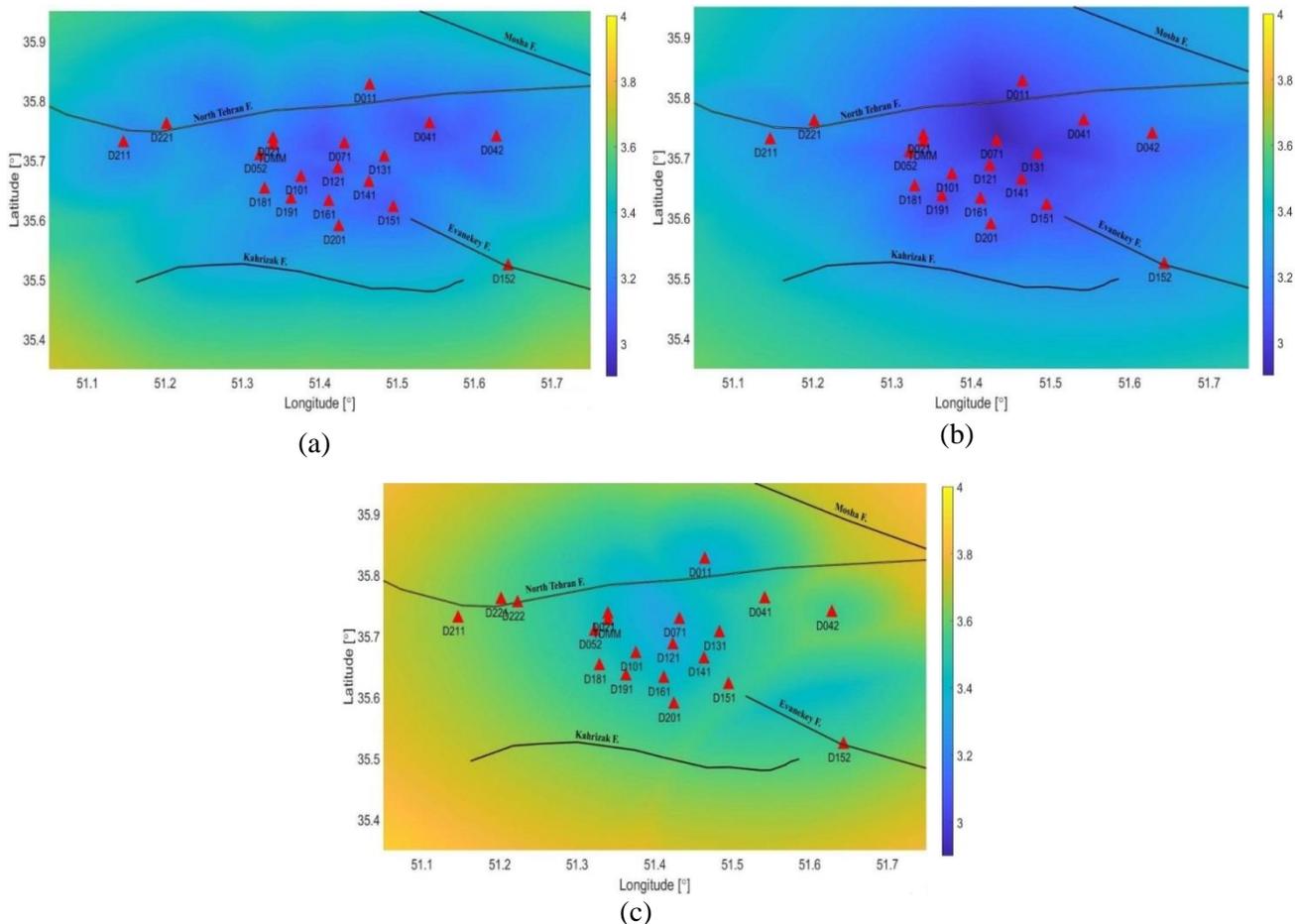
Figure 3. The detection threshold map at a depth of 10 km for the (a) E-component of the S-wave (b) N-component of the S-wave, and (c) Z-component of the P-wave.

(a)

(b)
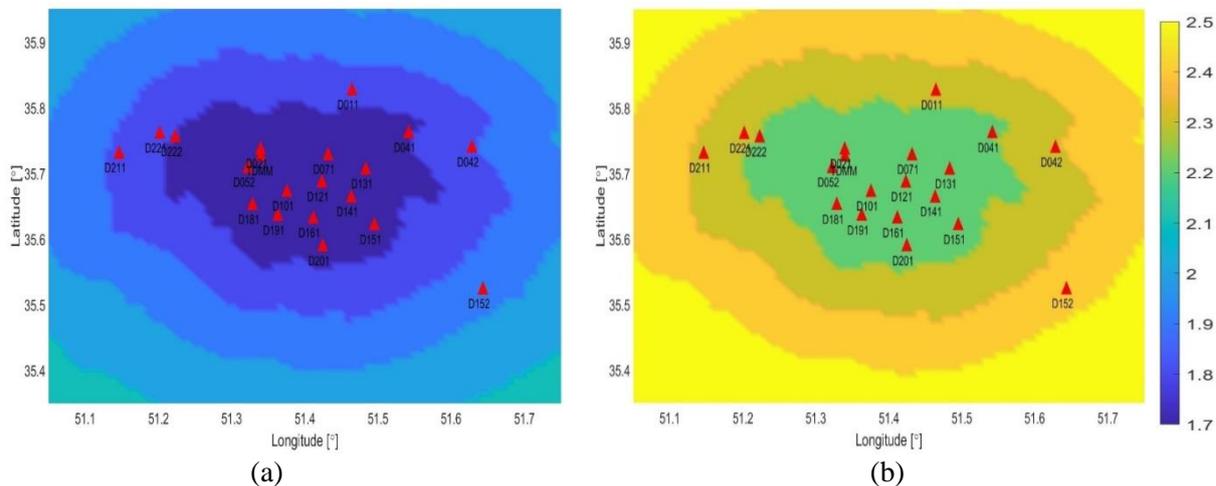
Figure 4. The detection threshold map with a constant noise level, station D071 as reference, at a depth of 10 km for (a) S-wave, and (b) P-wave.

4. Discussion

Several used parameters in this study are assumed steady inside the networks and fixed in comparing process of the Brune model with noise levels. However, such parameters are affected by uncertainties that may influence the detection threshold. Therefore,

the detection threshold variation is studied as a function of the reduced time (t^*), the stress drop ($\Delta\sigma$), and earthquake depths (Z), which are the most vital parameters in the definition of the Brune spectrum.

In this analysis, a magnitude referred to as the minimum detectable magnitude is plotted

as a function of investigated parameters (Figure 5). Conclusively, changes in the stress drop do not affect the minimum detectable magnitude of the network (Figure 5-a). Hence, to evaluate the detection threshold, averaged values even affected by large errors can be accepted for this parameter. Instead, changes in the focal depth from 5 to 20 km leads to changes of 0.3 units in the magnitude of the S- and P-waves (Figure 5-b), and also changes of t^* between 0.015 and 0.035 sec, resulting in changes in the threshold of 0.4 units in M_w (Figure 5-c). Therefore, a correct estimation of these two effective parameters is relevant for the evaluation of detection threshold.

5. Conclusion

Since the seismic waves recorded by near-surface sensors are usually combined with noise, the earthquake detection is calculated using the SNR method. The recorded seismic data is sometimes low quality, which is described as a low SNR. This low SNR of seismic data leads to a poor quality of many seismic analyzes, such as the detection threshold. Therefore, a minimum value of 5 is required to detect the S-wave on the horizontal components and the P-wave on the vertical components, and if at least five stations have this value, a seismic event could be located. Therefore, the smallest magnitude detectable events in the center of network at a depth of 10 km is 3.0 for S-waves and 3.3 for P-waves due to the geometry and stations' noise level of these two accelerometer networks.

(a)

(b)

(c)
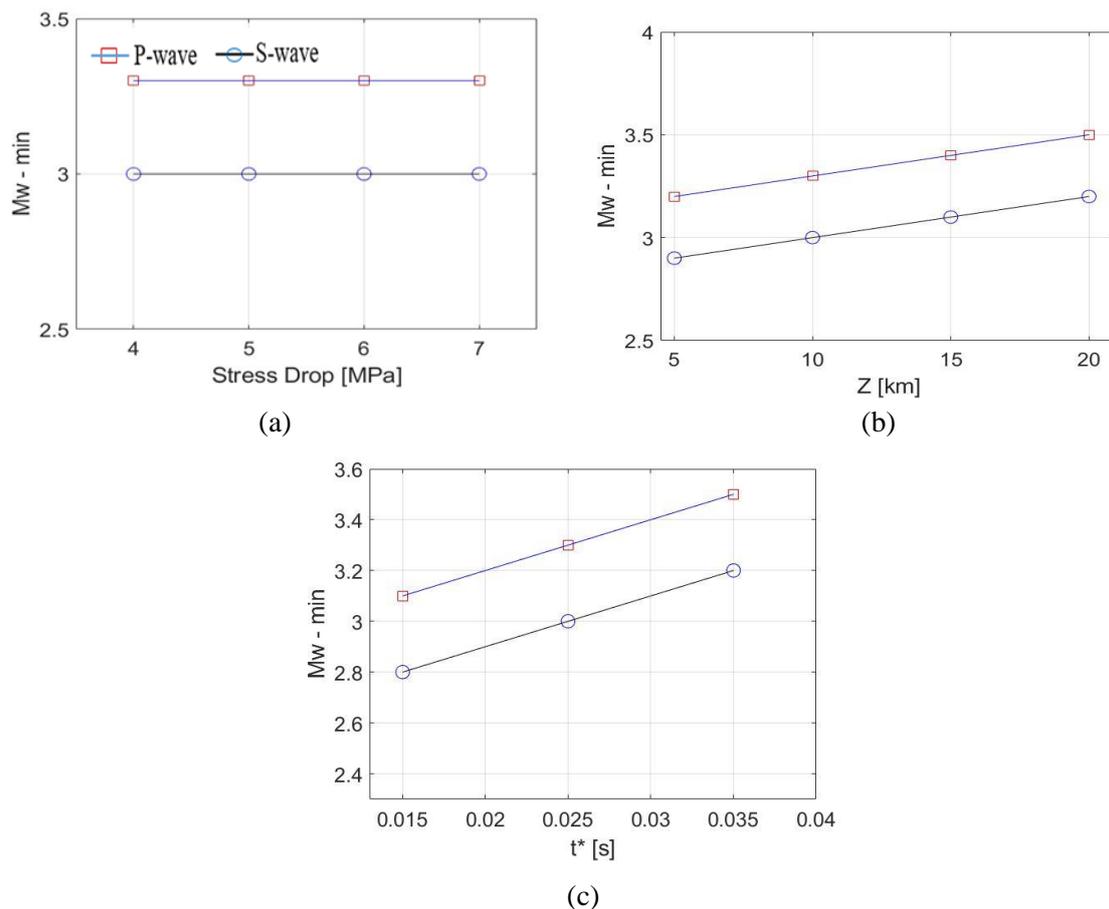
Figure 5. Variability of the detection threshold for P- and S-waves as a function of (a) the stress drop, (b) the focal depth, and (c) the reduced time (t^*). Changes in the stress drop do not affect the magnitude of the threshold (a), while changes in focal depth from 5 to 20 km cause changes as large as 0.3 units in magnitude of the threshold (b), and changes in t^* from 0.015 to 0.035 sec cause changes as large as 0.4 units in the magnitude of the threshold (c).

As the result shows, the accelerometers have not been able to detect micro earthquakes; however, it is expected that the borehole stations could be used for this purpose because of low noise level respect to those settled on the surface, which increases its detection capability. However, it is possible that the borehole sensors are overwhelmed when a strong earthquake occurs close by, in which case they are clipped and collected data practically become useless. Therefore, in order to detect earthquakes more accurately, it is better to place accelerometers around the wellhead of the borehole. Such accelerometers are actually strong motion sensors designed to record strong earthquakes with high fidelity. Therefore, it seems that the highly sensitive borehole sensor and surface accelerometer together are able to record the full spectrum of earthquakes.

Acknowledgment

References

Aki, K., & Richards, P.G. (1980). Quantitative Seismology: Theory and Methods. W. H. Freeman, San Francisco.

Atkinson, G.M. (1993). Earthquake source spectra in eastern north America. *Bulletin of the Seismological Society of America*, 83(6), 1778-1798.

Bobbio, A., Vassallo, M., & Festa, G. (2009). A local magnitude scale for southern Italy. Bulletin of the Seismological Society of *America*, 99(4), 2461-2470.

Boore, D. M., & Boatwright, J. (1984). Average body-wave radiation coefficients. *Bulletin of the Seismological Society of America*, 74(5), 1615-1621.

Brune, J. N. (1970). Tectonic stress and the spectra of seismic shear waves from earthquakes. *Journal of Geophysics*, 75, 4997-5009.

Brune, J. N. (1971). Tectonic stress and the spectra of seismic shear waves from earthquakes. *Journal of Geophysics*, 76,

5002.

Ding, L. (2015). Stress drop and its uncertainty for earthquakes M 3.8-5.5 in central California and Oklahoma. *M.Sc. thesis*, University of California.

Incorporated Research Institutions for Seismology. (2017). Software Downloads – PQLX, https://ds.iris.edu/ds/nodes/dmc/software/downloads/pqlx/.

Malagnini, L., & Dreger, D.S. (2016). Generalized free-surface effect and random vibration theory: a new tool for computing moment magnitudes of small earthquakes using borehole data. *Geophysical Journal International*, 206(1), 103-113.

Margheriti, L., & Zollo, A. (2010). High-resolution multi-disciplinary monitoring of active fault test-site areas in Italy, Final report S5-DPC-INGV Project, http://dcp-s5.rm.ingv.it/en/S5.html (last accessed October 2011), pp. 14.

Memarian, H., Kamranzad, F., & Zare, M. (2020). Earthquake risk assessment for Tehran, Iran. *International Journal of Geo-Information*, 430(9).

Ringdal, F. (1975). On the estimation of seismic detection thresholds. *Bulletin of the Seismological Society of America*, 65(6), 1631-1642.

Vassallo, M., Festa, G.F. & Bobbio, A. (2012). Seismic Ambient Noise Analysis in Southern Italy. *Bulletin of the Seismological Society of America*, 102(2), 574–586.

Weidle, C., Wenzel, F., & Ismail-Zadeh, A. (2006). t*- an unsuitable parameter to characterize anelastic attenuation in the Eastern Carpathians. *Geophysical Journal International*, 170(3), 1139-1150.

Yazdani, A., Kowsari, M., & Amani, S. (2016). Development of a regional attenuation relationship for Alborz, Iran. *Journal of the Earth and Space Physics*, 41(4), 39-50.

Zafarani, H., Ghorbani-Tanha, A.K., Rahimian, M., & Noorza, A. (2008). Seismic response analysis of Milad tower in Tehran, Iran, under site-specific simulated ground motions. *The 14th Worlds Conference on Earthquake Engineering*, Beijing, China.